Aicardi-Goutières Syndrome Is Caused by *IFIH1* Mutations

Hirotsugu Oda,[1,2] Kenji Nakagawa,[1] Junya Abe,[1,3] Tomonari Awaya,[1] Masahide Funabiki,[4] Atsushi Hijikata,[5] Ryuta Nishikomori,[1,*] Makoto Funatsuka,[6] Yusei Ohshima,[7] Yuji Sugawara,[8] Takahiro Yasumi,[1] Hiroki Kato,[4,9] Tsuyoshi Shirai,[5] Osamu Ohara,[2,10] Takashi Fujita,[4] and Toshio Heike[1]

Aicardi-Goutières syndrome (AGS) is a rare, genetically determined early-onset progressive encephalopathy. To date, mutations in six genes have been identified as etiologic for AGS. Our Japanese nationwide AGS survey identified six AGS-affected individuals without a molecular diagnosis; we performed whole-exome sequencing on three of these individuals. After removal of the common polymorphisms found in SNP databases, we were able to identify *IFIH1* heterozygous missense mutations in all three. In vitro functional analysis revealed that *IFIH1* mutations increased type I interferon production, and the transcription of interferon-stimulated genes were elevated. *IFIH1* encodes MDA5, and mutant MDA5 lacked ligand-specific responsiveness, similarly to the dominant *Ifih1* mutation responsible for the SLE mouse model that results in type I interferon overproduction. This study suggests that the *IFIH1* mutations are responsible for the AGS phenotype due to an excessive production of type I interferon.

Aicardi-Goutières syndrome (AGS [MIM 225750]) is a rare, genetically determined early-onset progressive encephalopathy.[1] Individuals affected with AGS typically suffer from progressive microcephaly associated with severe neurological symptoms, such as hypotonia, dystonia, seizures, spastic quadriplegia, and severe developmental delay.[2] On brain imaging, AGS is characterized by basal ganglia calcification, white matter abnormalities, and cerebral atrophy.[3,4] Cerebrospinal fluid (CSF) analyses show chronic lymphocytosis and elevated levels of IFN-α and neopterin.[3–5] AGS-affected individuals are often misdiagnosed as having intrauterine infections, such as TORCH syndrome, because of the similarities of these disorders, particularly the intracranial calcifications.[1] In AGS, etiological mutations have been reported in the following six genes: *TREX1* (MIM 606609), which encodes a DNA exonuclease; *RNASEH2A* (MIM 606034), *RNASEH2B* (MIM 610326), and *RNASEH2C* (MIM 610330), which together comprise the RNase H2 endonuclease complex; *SAMHD1* (MIM 606754), which encodes a deoxynucleotide triphosphohydrolase; and *ADAR1* (MIM 146920), which encodes an adenosine deaminase.[6–9] Although more than 90% of AGS-affected individuals harbor etiological mutations in one of these six genes, some AGS-affected individuals presenting with the clinical characteristics of AGS still lack a genetic diagnosis, suggesting the existence of additional AGS-associated genes.[1]

We recently conducted a nationwide survey of AGS in Japan and reported 14 AGS-affected individuals.[10] We have since recruited three other Japanese AGS-affected individuals, and among these 17 individuals, we have identified 11 individuals with etiologic mutations; namely, *TREX1* mutations in six, *SAMHD1* mutations in three, and *RNASEH2A* and *RNASEH2B* mutations in one each. Of the remaining six individuals without a molecular diagnosis, trio-based whole-exome sequencing was performed in three whose parents also agreed to participate in further genome-wide analyses (Figure 1A). Genomic DNA from each individual and the parents was enriched for protein-coding sequences, followed by massively parallel sequencing. The extracted nonsynonymous or splice-site variants were filtered to remove those with minor allele frequencies (MAF) > 0.01 in dbSNP137. To detect de novo variants, any variants observed in family members, listed in Human Genetic Variation Database (HGVD), or with MAF > 0.02 in our in-house exome database were removed. To detect autosomal-recessive (AR), compound heterozygous (CH), or X-linked (XL) variants, those with MAF > 0.05 in our in-house database were removed (Figure S1 available online). All samples were collected with the written informed consents by parents, and the study protocol was approved by the ethical committee of Kyoto University Hospital in accordance with the Declaration of Helsinki.

After common polymorphisms were removed, we identified a total of 40, 18, 89, and 22 candidate variants under the de novo, AR, CH, and XL inheritance models, respectively, that were present in at least one of the three individuals (Table S1). Among them, missense mutations were identified in *IFIH1* (MIM 606951, RefSeq accession

[1]Department of Pediatrics, Kyoto University Graduate School of Medicine, Kyoto 6068507, Japan; [2]Laboratory for Integrative Genomics, RIKEN Center for Integrative Medical Sciences, Yokohama 2300045, Japan; [3]Department of Pediatrics, Kitano Hospital, Tazuke Kofukai Medical Research Institute, Osaka 5308480, Japan; [4]Laboratory of Molecular Genetics, Institute for Virus Research, Kyoto University, Kyoto 6068507, Japan; [5]Department of Bioscience, Nagahama Institute of Bio-Science and Technology, Nagahama 5260829, Japan; [6]Department of Pediatrics, Tokyo Women's Medical University, Tokyo 1628666, Japan; [7]Department of Pediatrics, Faculty of Medical Sciences, University of Fukui, Fukui 9108507, Japan; [8]Department of Pediatrics and Developmental Biology, Graduate School of Medical and Dental Sciences, Tokyo Medical and Dental University, Tokyo 1138510, Japan; [9]Precursory Research for Embryonic Science and Technology (PRESTO), Science and Technology Agency (JST), Kawaguchi 3320012, Japan; [10]Department of Human Genome Research, Kazusa DNA Research Institute, Kisarazu 2920818, Japan
*Correspondence: rnishiko@kuhp.kyoto-u.ac.jp
http://dx.doi.org/10.1016/j.ajhg.2014.06.007.

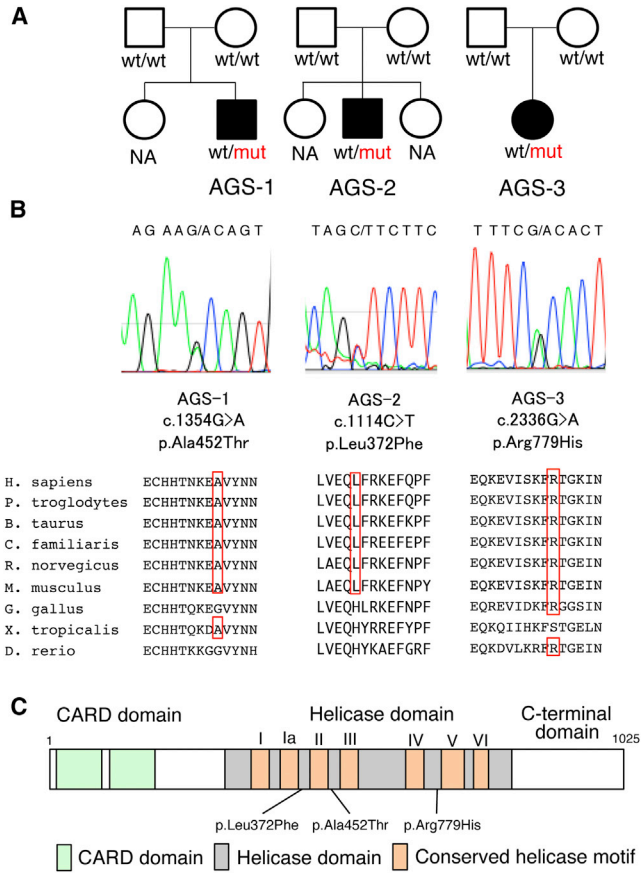

Figure 1. Pedigree Information for the AGS-Affected Individuals and Details of the *IFIH1* Mutations Identified

(A) The pedigrees of the three families indicating the AGS probands.

(B) Sanger sequencing chromatograms of the three *IFIH1* mutations found in the AGS-affected individuals. The locations of these mutations in the amino acid sequence of the MDA5 protein are shown in alignment with the conserved amino acid sequences from several species. This alignment was obtained via ClustalW2. The amino acids that are conserved with human are circled in red.

(C) The MDA5 protein domain structure with the amino acid substitutions observed in these AGS-affected individuals.

number NM_022168.2), which encodes MDA5 (RefSeq NP_071451.2). These missense mutations are c.1354G>A (p.Ala452Thr) in AGS-1; c.1114C>T (p.Leu372Phe) in AGS-2; and c.2336G>A (p.Arg779His) in AGS-3 (Figure 1B). None of the mutations are found in HGVD, including the 1,208 Japanese samples, or our in-house exome database of 312 Japanese individuals. Multiple-sequence alignment by ClustalW2 revealed that each of the amino acids affected by these mutations are conserved among mammals (Figure 1B). The subsequent amino acid alterations were all suggested to be disease causing in at least one of the four function-prediction programs used (Table 1). None of the other genes identified in the de novo inheritance model, or any of the genes identified in the other three inheritance models, were mutated in all three individuals. The *IFIH1* mutations identified were validated by Sanger sequencing. The other coding exons of *IFIH1* were also examined by Sanger sequencing, and no other mutations were found.

MDA5 is one of the cytosolic pattern recognition receptors that recognizes double-stranded RNA (dsRNA).[11] MDA5 consists of N-terminal tandem CARD domains, a central helicase domain, and a C-terminal domain (Figure 1C). When bound to dsRNA, MDA5 forms a closed, C-shaped ring structure around the dsRNA stem and excludes the tandem CARD as well as creates filamentous oligomer on dsRNA.[12] It is hypothesized that the tandem CARD interacts each other and activates MAVS on the mitochondrial outer membrane. Oligomerization of MAVS induces TBK1 activation, IRF3 phosphorylation, and induction of type I interferon transcription, resulting in the activation of a large number of interferon-stimulated genes (ISGs).

The neurological findings of the individuals with these *IFIH1* mutations are typical of AGS (Table S2). They were born with appropriate weights for their gestational ages without any signs of intrauterine infection. However, they all demonstrated severe developmental delay in early infancy associated with progressive microcephaly. No arthropathy, hearing loss, or ophthalmological problems were observed. As for extraneural features, all three individuals had at least one of the following autoimmune features: positivity for autoantibodies, hyperimmunoglobulinemia, hypocomplementemia, and thrombocytopenia. Notably, none of the individuals with *IFIH1* mutations had chilblain lesions, although all the five individuals with *TREX1* mutations and two of the three individuals with *SAMHD1* mutations in the Japanese AGS cohort showed chilblain lesions.[10] Individuals with *SAMHD1* mutations and *IFIH1* mutations both show autoimmune features; however, chilblain lesions have been observed only in individuals with *SAMHD1* mutations.[10]

To predict the effects of the identified amino acid substitutions on MDA5, three-dimensional model structures of MDA5 mutants were generated from the crystal structure of human MDA5-dsRNA complex[12] (Protein Data Bank [PDB] code 4gl2), using PyMOL (Schroedinger) and MOE (Chemical Computing Group) (Figure S2A). The oligomeric model of MDA5 was generated using the electron microscopy imaging data of MDA5 filament lacking CARD domain[13] (Electron Microscopic Data Bank [EMDB] code 5444) (Figure S2B). The three amino acid substitutions in the AGS-affected individuals are all located within the helicase domain (Figures 1C and S2A). Because Ala452 directly contacts the dsRNA ribose O2′ atom, the p.Ala452Thr substitution probably affects the binding affinity to dsRNA due to an atomic repulsion between the side chain of Thr452 and the dsRNA O2′ atom (Figures S2C and S2D). Leu372 is located adjacent to the ATP binding pocket, and the p.Leu372Phe substitution could increase the side chain volume of the binding pocket, affecting its ATP hydrolysis activity (Figures S2E and S2F). In our oligomeric model, Arg779 is located at the interface between the two monomers, which is consistent with the

Table 1. Functional Predictions of the *IFIH1* Variants

Individuals	Nucleotide Change	Amino Acid Change	SIFT	PolyPhen2	Mutation Taster	PROVEAN
AGS-1	c.1354G>A	p.Ala452Thr	tolerated	benign	disease causing	neutral
AGS-2	c.1114C>T	p.Leu372Phe	tolerated	probably damaging	disease causing	neutral
AGS-3	c.2336G>A	p.Arg779His	tolerated	probably damaging	disease causing	deleterious

The potential functional effects of the *IFIH1* variants identified in the AGS-affected individuals were predicted via SIFT, PolyPhen2, Mutation Taster, and PROVEAN.

recent report showing that Lys777, close to Arg779, is in close proximity to the adjacent monomer.[12] Furthermore, in our model, Arg779 is in close to Asp572 on the surface of the adjacent monomer. We speculate that losing the positive charge due to the p.Arg779His substitution would possibly affect the electrostatic interaction between the MDA5 monomers (Figures S2G and S2H).

To connect the identified *IFIH1* mutations with the AGS phenotype, we examined the type I interferon signature in the individuals by performing quantitative RT-PCR (qRT-PCR) of seven ISGs.[14] Peripheral blood mononuclear cells (PBMCs) from the three AGS-affected individuals showed upregulation of ISG transcription (Figure 2), confirming the type I interferon signature in the individuals with *IFIH1* mutations.

To elucidate the disease-causing capability of the identified *IFIH1* mutations, three FLAG-tagged *IFIH1* mutant plasmids containing these mutations were constructed via site-directed mutagenesis. These plasmids were transiently expressed on human hepatoma cell line Huh7 and the *IFNB1* promoter activity as well as endogenous expression of *IFIT1* (MIM 147690) was measured 48 hr after transfection.[15] The three mutant plasmids activated the *IFNB1* promoter in Huh7 cells more strongly than the wild MDA5 and nearby missense variants reported in dbSNP (Figures 3 and S3). The upregulation of endogenous *IFIT1* was also observed in the transfected cells (Figure S4), suggesting that these AGS mutations enhance the intrinsic activation function of MDA5. Recent genome-wide association studies (GWASs) showed association of the *IFIH1* with various autoimmune diseases, such as systemic lupus erythematosus (SLE), type I diabetes, psoriasis, and vitiligo.[16–19] We examined *IFNB1* promoter activity induced by the c.2836G>A (p.Ala946Thr) polymorphism (rs1990760) identified in the GWASs. Although the c.2836G>A polymorphism partially activated the promoter activity, the induced activity was lower than those of the AGS-derived mutants. In addition, the dominantly inherited SLE mouse model in the ENU-treated mouse colony is reported to have the *Ifih1* mutation, c.2461G>A (p.Gly821Ser).[15] These observations suggest that *IFIH1* has strong association with various autoimmune diseases, especially SLE, which also has a type I interferon signature.[20] Because alteration of *TREX1* has been reported to cause AGS as well as SLE,[21] it seems quite plausible for *IFIH1* to also be involved in both AGS and SLE. Interestingly, all the individuals identified with *IFIH1* mutations had autoantibodies, suggesting the contribution of *IFIH1* mutations to autoimmune phenotypes.

To further delineate the functional consequences of the three *IFH1* mutations, we measured the ligand-specific *Ifnb* mRNA induction by stimulating *Ifih1*^{null} mouse embryonic fibroblasts (MEFs) reconstituted with retrovirus expressing the *IFIH1* mutants by an MDA5-specific ligand, encephalomyocarditis virus (EMCV).[22] None of the MEF cells expressing the three mutant *IFIH1* responded to the EMCV, which suggested that the MDA5 variants lacked the ligand-specific responsiveness. The response of the three AGS mutants against the MDA5-specific EMCV was similar to that of the p.Gly821Ser variant reported in the dominantly inherited SLE mouse model with type I interferon overproduction[15] (Figures 4 and S5).

During the revision of this manuscript, Rice et al. identified nine individuals with *IFIH1* mutations, including the c.2336G>A mutation we identified, in a spectrum of neuroimmunological features consistently associated with enhanced type I interferon states including AGS.[23] Although we agree that the *IFIH1* mutations cause constitutive type I interferon activation, Rice et al. show that the mutated MDA5 proteins maintain ligand-induced responsiveness, which was not the case in our study. Because we measured the ligand-specific responsiveness of MDA5 in different experimental conditions, further analysis remains to be performed to reveal the biochemical mechanism of interferon overproduction by the mutated MDA5.

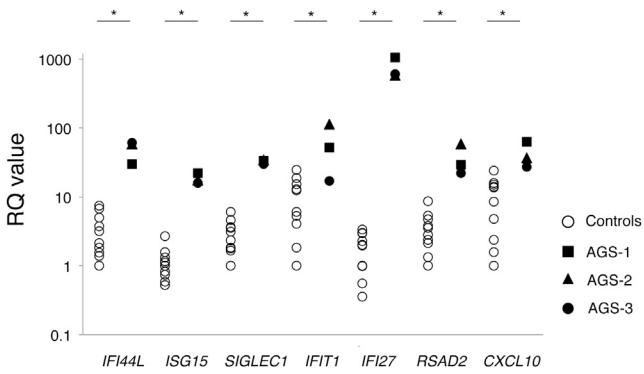

Figure 2. Quantitative RT-PCR of a Panel of Seven ISGs in PBMCs Obtained from the *IFIH1*-Mutated Individuals and Healthy Control Subject

qRT-PCR was performed as previously described.[15] The relative abundance of each transcript was normalized to the expression level of β-actin. Taqman probes used were the same as previous report,[14] except for *ACTB* (MIM 102630). Individual data were shown relative to a single calibrator (control 1). The experiment was performed in triplicate. Statistical significance was determined by Mann-Whitney U test, *$p < 0.05$.

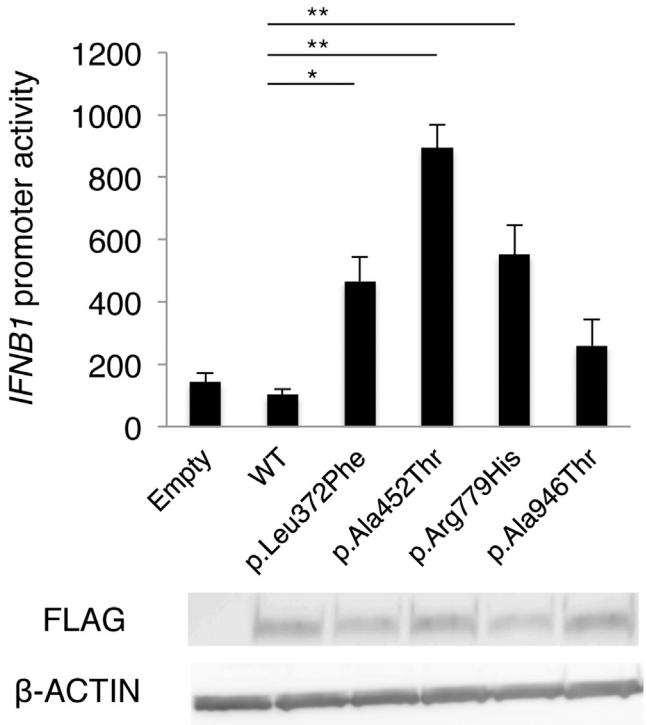

Figure 3. The Effects of the Three MDA5 Variants on *IFNB1* Expression

Huh7 cells were transfected with a reporter gene containing *IFNB1* promoter (p-55C1B Luc), an empty vector (BOS), and expression vectors for FLAG-tagged human wild-type *IFIH1*, c.2836G>A polymorphism (p.Ala946Thr) in the GWASs, and the identified *IFIH1* mutants. Luciferase activity was measured 48 hr after transfection, and the MDA5 protein accumulation was examined by immunoblotting as previously described.[15] FLAG indicates the accumulation of FLAG-tagged MDA5. Each experiment was performed in triplicate and data are mean ± SEM. Shown is a representative of two with consistent results. Statistical significance was determined by Student's t test. *$p < 0.05$, **$p < 0.01$.

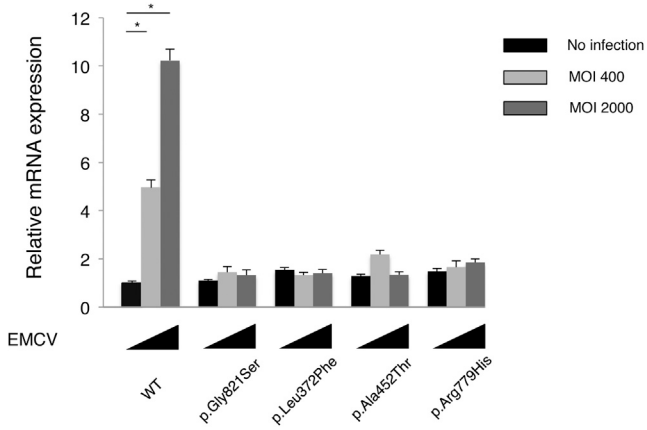

Figure 4. *Ifnb* mRNA Levels in *Ifih1*-Deficient MEFs Expressing *IFIH1* Mutants

The MEFs were infected with retroviruses encoding mouse wild-type *Ifih1*, mouse *Ifih1* with c.2461G>A (p.Gly821Ser) (RefSeq NM_027835.3) mutation, or the three AGS mutants of human *IFIH1*. At 48 hr after the retroviral infection, these MEFs were infected with indicated multiplicity of infection (MOI) of EMCV for 6 hr, and *Ifnb* mRNA levels were measured by qRT-PCR. The relative abundance of each transcript was normalized to the expression level of 18S ribosomal RNA. Data are shown as mean ± SEM of triplicate samples. Shown is a representative of two independent experiments. Statistical significance was determined by Student's t test, *$p < 0.001$. The expression of the retrovirally transduced FLAG-tagged constructs was confirmed by immunoblotting (Figure S5).

In conclusion, we identified mutations in *IFIH1* as a cause of AGS. The individuals with the *IFIH1* mutations showed encephalopathy typical of AGS as well as the type I interferon signature with autoimmune phenotypes, but lacked the chilblains. Further analysis remains to elucidate the mechanism of how the *IFIH1* mutations identified in AGS cause the type I interferon overproduction.

Supplemental Data

Supplemental Data include five figures and two tables and can be found with this article online at http://dx.doi.org/10.1016/j.ajhg.2014.06.007.

Acknowledgments

We are very grateful to Y. Takaoka (Kyoto University) and E. Abe (RIKEN Center for Integrative Medical Sciences) for their technical assistance on Sanger sequencing, to E. Hirano (Kyoto University) for her technical assistance on functional analyses of the AGS mutants, to M. Takazawa (Kazusa DNA Research Institute) for his contribution to exome data analysis, and to T. Taylor for his critical reading of the manuscript. This work was supported by the Platform for Drug Discovery, Informatics, and Structural Life Science from the Ministry of Education, Culture, Sports, Science and Technology, Japan. This work was supported by Grants-in-aid for Scientific Research from the Japanese Ministry of Health, Labor and Welfare and the Japanese Ministry of Education, Culture, Sports, Science, Technology (MEXT).

Received: March 1, 2014
Accepted: June 11, 2014
Published: July 3, 2014

Web Resources

The URLs for the data presented herein are as follows:

Burrows-Wheeler Aligner, http://bio-bwa.sourceforge.net/
ClustalW2, http://www.ebi.ac.uk/Tools/msa/clustalw2/
dbSNP, http://www.ncbi.nlm.nih.gov/projects/SNP/
EMDataBank, http://www.emdatabank.org/index.html
GATK, http://www.broadinstitute.org/gatk/
Human Genetic Variation Database (HGVD), http://www.genome.med.kyoto-u.ac.jp/SnpDB/
MutationTaster, http://www.mutationtaster.org/
Online Mendelian Inheritance in Man (OMIM), http://www.omim.org/
PolyPhen-2, http://www.genetics.bwh.harvard.edu/pph2/
PROVEAN, http://provean.jcvi.org/index.php
RCSB Protein Data Bank, http://www.rcsb.org/pdb/home/home.do
RefSeq, http://www.ncbi.nlm.nih.gov/RefSeq
SIFT, http://sift.bii.a-star.edu.sg/

References

1. Chahwan, C., and Chahwan, R. (2012). Aicardi-Goutieres syndrome: from patients to genes and beyond. Clin. Genet. *81*, 413–420.
2. Ramantani, G., Kohlhase, J., Hertzberg, C., Innes, A.M., Engel, K., Hunger, S., Borozdin, W., Mah, J.K., Ungerath, K., Walkenhorst, H., et al. (2010). Expanding the phenotypic spectrum of lupus erythematosus in Aicardi-Goutières syndrome. Arthritis Rheum. *62*, 1469–1477.
3. Orcesi, S., La Piana, R., and Fazzi, E. (2009). Aicardi-Goutieres syndrome. Br. Med. Bull. *89*, 183–201.
4. Rice, G., Patrick, T., Parmar, R., Taylor, C.F., Aeby, A., Aicardi, J., Artuch, R., Montalto, S.A., Bacino, C.A., Barroso, B., et al. (2007). Clinical and molecular phenotype of Aicardi-Goutieres syndrome. Am. J. Hum. Genet. *81*, 713–725.
5. Blau, N., Bonafé, L., Krägeloh-Mann, I., Thöny, B., Kierat, L., Häusler, M., and Ramaekers, V. (2003). Cerebrospinal fluid pterins and folates in Aicardi-Goutières syndrome: a new phenotype. Neurology *61*, 642–647.
6. Crow, Y.J., Hayward, B.E., Parmar, R., Robins, P., Leitch, A., Ali, M., Black, D.N., van Bokhoven, H., Brunner, H.G., Hamel, B.C., et al. (2006). Mutations in the gene encoding the 3′-5′ DNA exonuclease TREX1 cause Aicardi-Goutières syndrome at the AGS1 locus. Nat. Genet. *38*, 917–920.
7. Crow, Y.J., Leitch, A., Hayward, B.E., Garner, A., Parmar, R., Griffith, E., Ali, M., Semple, C., Aicardi, J., Babul-Hirji, R., et al. (2006). Mutations in genes encoding ribonuclease H2 subunits cause Aicardi-Goutières syndrome and mimic congenital viral brain infection. Nat. Genet. *38*, 910–916.
8. Rice, G.I., Bond, J., Asipu, A., Brunette, R.L., Manfield, I.W., Carr, I.M., Fuller, J.C., Jackson, R.M., Lamb, T., Briggs, T.A., et al. (2009). Mutations involved in Aicardi-Goutières syndrome implicate SAMHD1 as regulator of the innate immune response. Nat. Genet. *41*, 829–832.
9. Rice, G.I., Kasher, P.R., Forte, G.M., Mannion, N.M., Greenwood, S.M., Szynkiewicz, M., Dickerson, J.E., Bhaskar, S.S., Zampini, M., Briggs, T.A., et al. (2012). Mutations in ADAR1 cause Aicardi-Goutières syndrome associated with a type I interferon signature. Nat. Genet. *44*, 1243–1248.
10. Abe, J., Nakamura, K., Nishikomori, R., Kato, M., Mitsuiki, N., Izawa, K., Awaya, T., Kawai, T., Yasumi, T., Toyoshima, I., et al. (2014). A nationwide survey of Aicardi-Goutieres syndrome patients identifies a strong association between dominant TREX1 mutations and chilblain lesions: Japanese cohort study. Rheumatology *53*, 448–458.
11. Yoneyama, M., and Fujita, T. (2009). RNA recognition and signal transduction by RIG-I-like receptors. Immunol. Rev. *227*, 54–65.
12. Wu, B., Peisley, A., Richards, C., Yao, H., Zeng, X., Lin, C., Chu, F., Walz, T., and Hur, S. (2013). Structural basis for dsRNA recognition, filament formation, and antiviral signal activation by MDA5. Cell *152*, 276–289.
13. Berke, I.C., Yu, X., Modis, Y., and Egelman, E.H. (2012). MDA5 assembles into a polar helical filament on dsRNA. Proc. Natl. Acad. Sci. USA *109*, 18437–18441.
14. Rice, G.I., Forte, G.M., Szynkiewicz, M., Chase, D.S., Aeby, A., Abdel-Hamid, M.S., Ackroyd, S., Allcock, R., Bailey, K.M., Balottin, U., et al. (2013). Assessment of interferon-related biomarkers in Aicardi-Goutières syndrome associated with mutations in TREX1, RNASEH2A, RNASEH2B, RNASEH2C, SAMHD1, and ADAR: a case-control study. Lancet Neurol. *12*, 1159–1169.
15. Funabiki, M., Kato, H., Miyachi, Y., Toki, H., Motegi, H., Inoue, M., Minowa, O., Yoshida, A., Deguchi, K., Sato, H., et al. (2014). Autoimmune disorders associated with gain of function of the intracellular sensor MDA5. Immunity *40*, 199–212.
16. Smyth, D.J., Cooper, J.D., Bailey, R., Field, S., Burren, O., Smink, L.J., Guja, C., Ionescu-Tirgoviste, C., Widmer, B., Dunger, D.B., et al. (2006). A genome-wide association study of nonsynonymous SNPs identifies a type 1 diabetes locus in the interferon-induced helicase (IFIH1) region. Nat. Genet. *38*, 617–619.
17. Gateva, V., Sandling, J.K., Hom, G., Taylor, K.E., Chung, S.A., Sun, X., Ortmann, W., Kosoy, R., Ferreira, R.C., Nordmark, G., et al. (2009). A large-scale replication study identifies TNIP1, PRDM1, JAZF1, UHRF1BP1 and IL10 as risk loci for systemic lupus erythematosus. Nat. Genet. *41*, 1228–1233.
18. Strange, A., Capon, F., Spencer, C.C., Knight, J., Weale, M.E., Allen, M.H., Barton, A., Band, G., Bellenguez, C., Bergboer, J.G., et al.; Genetic Analysis of Psoriasis Consortium & the Wellcome Trust Case Control Consortium 2 (2010). A genome-wide association study identifies new psoriasis susceptibility loci and an interaction between HLA-C and ERAP1. Nat. Genet. *42*, 985–990.
19. Jin, Y., Birlea, S.A., Fain, P.R., Ferrara, T.M., Ben, S., Riccardi, S.L., Cole, J.B., Gowan, K., Holland, P.J., Bennett, D.C., et al. (2012). Genome-wide association analyses identify 13 new susceptibility loci for generalized vitiligo. Nat. Genet. *44*, 676–680.
20. Bennett, L., Palucka, A.K., Arce, E., Cantrell, V., Borvak, J., Banchereau, J., and Pascual, V. (2003). Interferon and granulopoiesis signatures in systemic lupus erythematosus blood. J. Exp. Med. *197*, 711–723.
21. Lee-Kirsch, M.A., Gong, M., Chowdhury, D., Senenko, L., Engel, K., Lee, Y.A., de Silva, U., Bailey, S.L., Witte, T., Vyse, T.J., et al. (2007). Mutations in the gene encoding the 3′-5′ DNA exonuclease TREX1 are associated with systemic lupus erythematosus. Nat. Genet. *39*, 1065–1067.
22. Kato, H., Takeuchi, O., Sato, S., Yoneyama, M., Yamamoto, M., Matsui, K., Uematsu, S., Jung, A., Kawai, T., Ishii, K.J., et al. (2006). Differential roles of MDA5 and RIG-I helicases in the recognition of RNA viruses. Nature *441*, 101–105.
23. Rice, G.I., del Toro Duany, Y., Jenkinson, E.M., Forte, G.M., Anderson, B.H., Ariaudo, G., Bader-Meunier, B., Baildam, E.M., Battini, R., Beresford, M.W., et al. (2014). Gain-of-function mutations in IFIH1 cause a spectrum of human disease phenotypes associated with upregulated type I interferon signaling. Nat. Genet. *46*, 503–509.

The American Journal of Human Genetics, Volume *95*

Supplemental Data

Aicardi-Goutières Syndrome Is Caused by *IFIH1* Mutations

Hirotsugu Oda, Kenji Nakagawa, Junya Abe, Tomonari Awaya, Masahide Funabiki, Atsushi Hijikata, Ryuta Nishikomori, Makoto Funatsuka, Yusei Ohshima, Yuji Sugawara, Takahiro Yasumi, Hiroki Kato, Tsuyoshi Shirai, Osamu Ohara, Takashi Fujita, and Toshio Heike

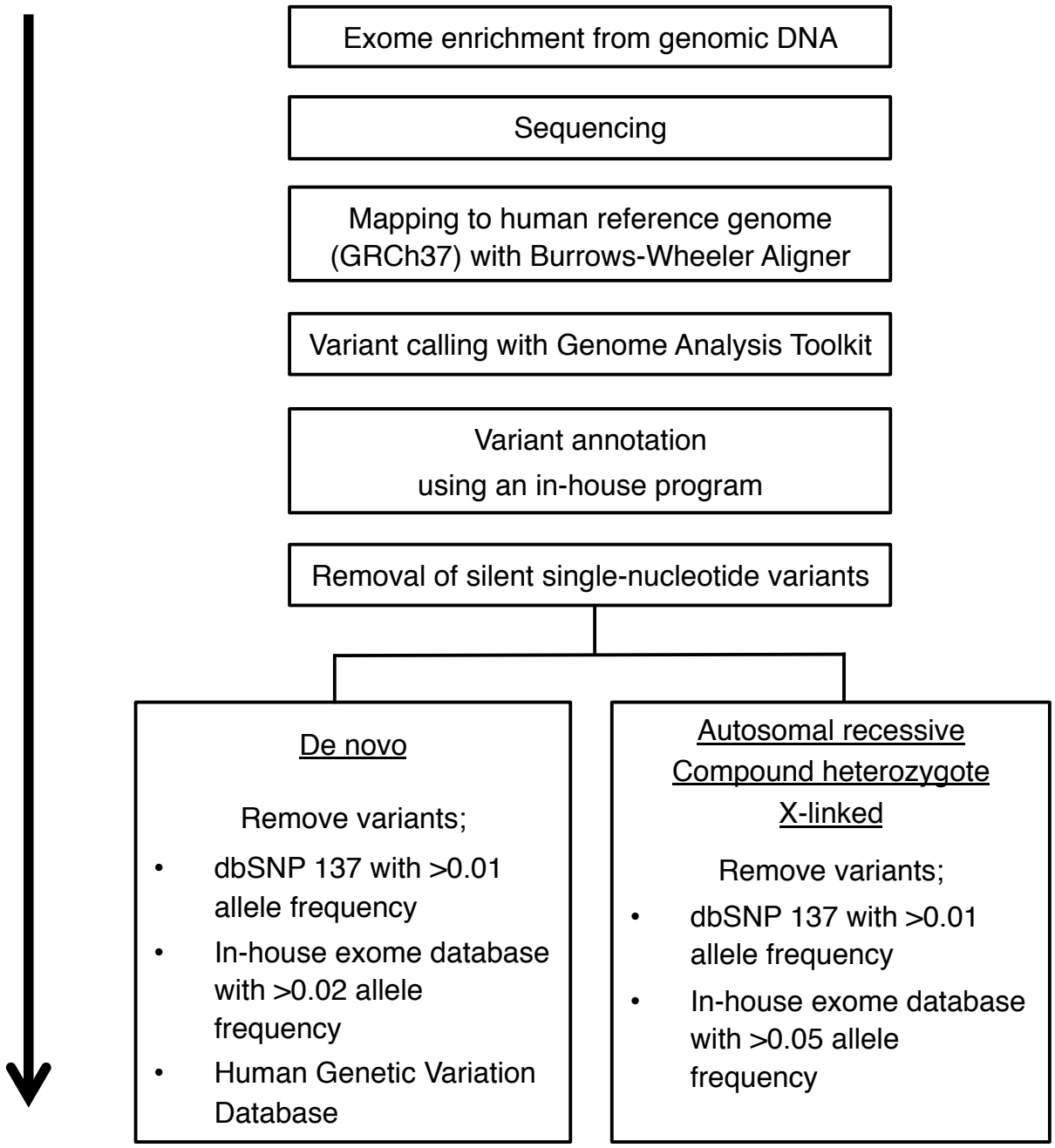

Figure S1. A flow diagram of the trio-based whole exome sequencing process.
GRCh37; Genome Reference Consortium Human build 37.

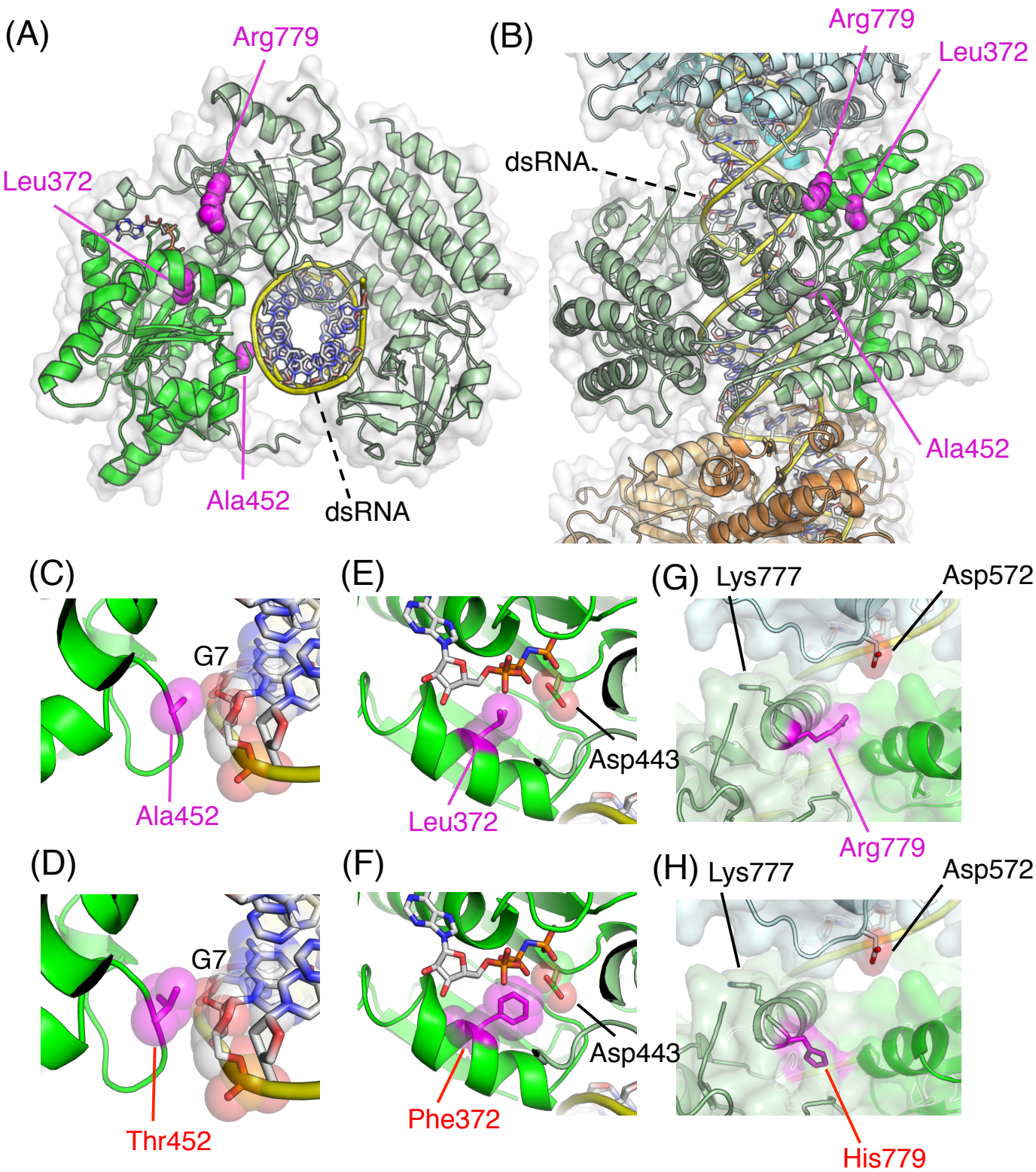

Figure S2. Predicted effects of MDA5 amino acid substitutions on its protein structure.

(A, B) Mapping of the three mutated amino acids on the crystal structure of MDA5-dsRNA complex (Protein Data Bank (PDB) code; 4gl2). The ATP-binding domain and the other domains of MDA5 are colored green and light-green, while the adjacent MDA5 monomers are colored light blue and orange, respectively. Three residues mutated in the patients, Ala452, Leu372, and Arg779, are shown in space filling models (magenta). (A) Top view of the tertiary structure of the MDA5 protein and dsRNA. (B) Side view of the model of MDA5 monomer oligomerization. The model was constructed by fitting the MDA5 monomers and the 38bps dsRNA structure into the density map from the electron microscopic analysis of the MDA5-dsRNA fibril (EMDB code; 5444).

(C, D, E, F, G, H) Detailed views of the mutated amino acid resides. (C) Ala452 is directly in contact with the O2’ atom of the ribose moiety of guanine residue (G7). (D) The p.Ala452Thr substitution is predicted to induce an electric repulsion between the side chain of Thr452 and the O2’ atom of RNA. (E) Leu372 is located in the ATP binding pocket. (F) The p.Leu372Phe substitution is predicted to increase the side chain volume of the binding pocket, and would affect the ATP hydrolysis activity of MDA5 by interfering with Asp443, a part of the catalytic residues. (G) Arg779 is located in the interface between MDA5 monomers, and is possibly involved in electrostatic interactions between the monomers. (H) The p.Arg779His substitution is predicted to affect the electrostatic interaction due to loss of the positive charge.

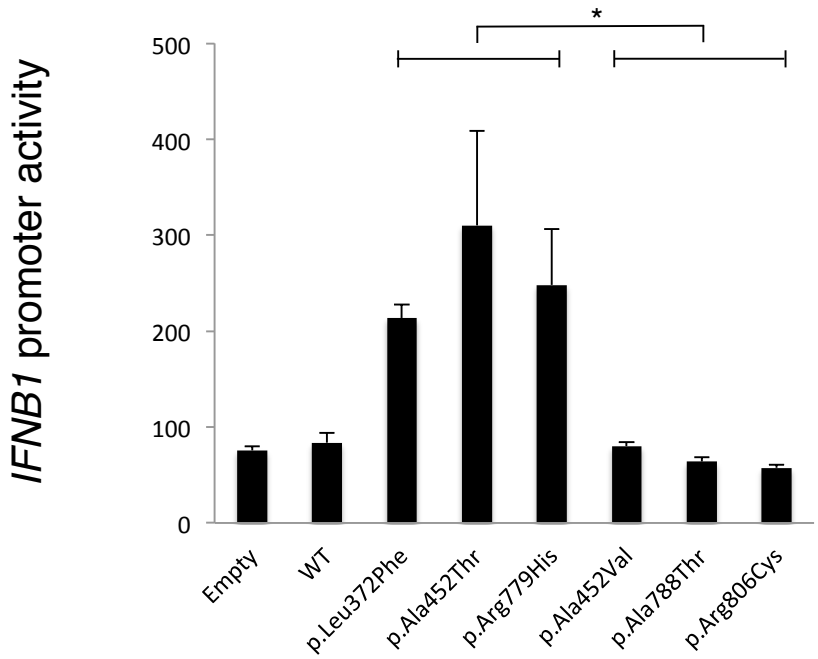

Figure S3. Comparison of the mutant MDA5 reporter activity between the AGS mutants and SNPs. Huh7 cells were transfected with a reporter gene containing *IFNB1* promoter (p-55C1B Luc), along with empty vector, wild-type MDA5, its three AGS mutants, or three MDA5 amino acid variations corresponding to other non-synonymous SNPs; namely, p.Ala452Val (c.1355C>T), p.Ala788Thr (2362G>A), and p.Arg806Cys (c.2416C>T). Luciferase activity was measured 48 hours after transfection. The experiment was performed in triplicate and data are mean ± S.E.M. The mean of each triplicate was compared between the three AGS mutants and three mutants having other SNPs. Statistical significance was determined by Student's *t*-test. **p*<0.005.

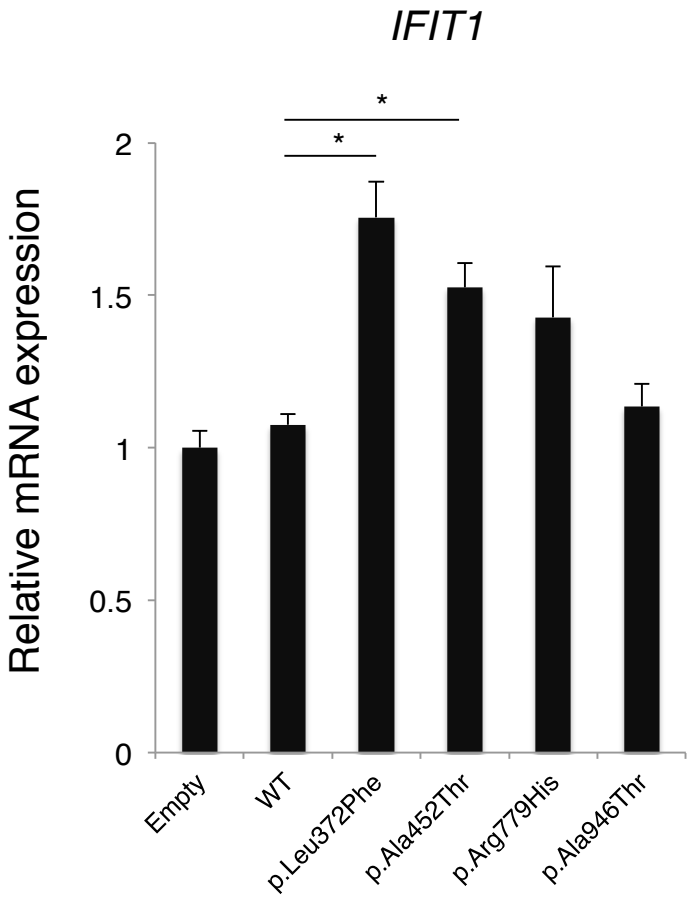

Figure S4. Endogenous expression of the *IFIT1* gene in the Huh7 transfection. *IFIT1* expression of the transfected Huh7 cells was measured by RT-qPCR. The relative abundance of each transcript was normalized to the expression level of 18S ribosomal RNA. Each experiment was performed in triplicate and data are mean ± S.E.M. Statistical significance was determined by Student's *t*-test. *$p<0.01$.

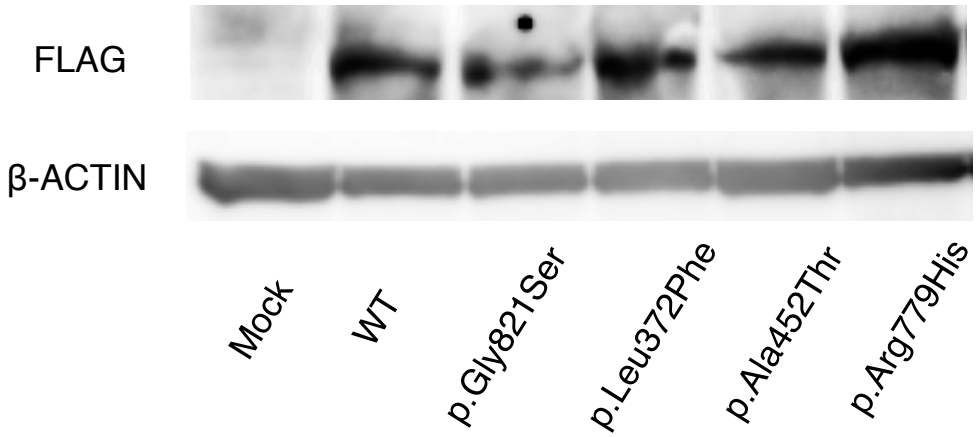

Figure S5. Retrovirally transduced expression of *IFIH1* constructs in *Ifih1*^{null} MEFs.

Ifih1^{null} MEFs were transfected with empty retrovirus vector, retrovirus encoding FLAG-mouse wild type *Ifih1* (WT) or FLAG-mouse *Ifih1* with p.Gly821Ser mutation, or the FLAG-tagged three AGS mutants of human *IFIH1*. The FLAG-tagged MDA5 and β-Actin accumulation was examined by Western blotting.

Supplemental table 1

Exome sequencing summary

	AGS-1	AGS-2	AGS-3
Exome enrichment kit	Illumina TruSeq Exome Enrichment Kit	Illumina TruSeq Exome Enrichment Kit	Agilent SureSelect Human All Exon V5 Kit
Sequencer	HiSeq 1000	HiSeq 1000	HiSeq 1500
Mapped region (>=5x)	58384949	57380736	87233940
Exome target region	62286366	62286366	89659527
>=x5 coverage (%)	93.7363	92.1240	97.2946
Total variants	60273	57558	99557

Variants after dbSNP137 filtering	AGS-1	AGS-2	AGS-3
Total	2804	2622	2522
Frameshift	111	98	114
Nonsense	51	50	47
Missense or in-frame indel	2618	2454	2067
Splice-site	24	20	294

Rare variants	AGS-1	AGS-2	AGS-3
Total	34	28	102
De novo	7	4	28
Autosomal recessive	5	2	11
Compound heterozygous	12	10	63
X-linked	10	12	N.D.

Sequence data were mapped against the human reference genome (Genome Reference Consortium Human Build 37) using Burrows-Wheeler Aligner software. Variants were called using the Genome Analysis Toolkit, and were filtered to remove those with variant quality scores less than 50. Gene annotation of each variant was performed using an in-house program. Identified non-synonymous or splice-site variants were filtered to remove those with minor allele frequencies (MAF) >0.01 in dbSNP137. For detecting any rare de novo variants, these variants observed in family members, identified in Human Genetic Variation Database, or those with MAF >0.02 in our in-house exome database were removed. For rare autosomal recessive, compound heterozygous, or X-linked variants, those with MAF >0.05 in our in-house database were removed. N.D.; not determined.

Supplemental table 2 Profiles of the AGS individuals

Clinical findings

	Age	Sex	GA	BW	Disease onset	Developmental delay	Other neurological manifestations	Chilblain lesions	Extraneural manifestations
AGS-1	5 yr	M	36 wk	2780 g	4 d Omphalitis with thrombocytopenia	Severe	Hypertonia, complex febrile seizure, microcephaly, spastic quadriplegia	No	Idiopathic interstitial pneumonia
AGS-2	6 yr	M	39 wk	3290 g	6 mo Developmental delay	Severe	Regression, dystonia, microcephaly, quadriplegia	No	Atopic dermatitis
AGS-3	2 yr	F	37 wk	2515 g	5 mo Developmental delay	Severe	Complex febrile seizure, dystonia, hypotonia, progressive microcephaly, spastic quadriplegia	No	Recurrent otitis media, sinusitis, periodic fever

Laboratory and radiographic findings

	CSF lymphocytosis	CSF elevated IFN-α	CSF elevated neopterin	Serum elevated autoantibody	Other laboratory features	Cranial calcification	White matter abnormality	Brain atrophy
AGS-1	No (16 mo)	Yes 13.2IU/ml (16 mo)	n.d.	Anti-LKM1	Thrombocytopenia, increased serum transaminases, hypocomplementemia, hypergammaglobulinemia	Yes Bilateral in the basal ganglia and white matter	Yes	Yes
AGS-2	No (3 yr)	No (3 yr)	Yes 285nM (3 yr)	ANA 1:320	None	Yes Bilateral in the basal ganglia and corticomedullary junction	Yes	Yes
AGS-3	No (12 mo)	No <6IU/ml (12 mo)	Yes 71.23nM (12 mo)	ANA 1:320 Anti-dsDNA Anti-Sm PAIgG	Thrombocytopenia, increased serum transaminases, hypocomplementemia, hypergammaglobulinemia	Yes Bilateral spotty in the basal ganglia and subcortical white matter	Yes	Yes

Notes: GA, gestational age; BW, birth weight; M, male; F, female; d, day(s); wk, week(s); mo, month(s); yr, year(s); n.d., not done.

The upper limit of normal CSF neopterin in our institute is 34.6nM at an age of 1-12 months and 25nM at an age of 2-12 years